Available online at www.sciencedirect.com
ScienceDirect
Journal of Catalysis 252 (2007) 178–189
JOURNAL OF CATALYSIS
www.elsevier.com/locate/jcat

Decatungstate catalyst supported on silica and γ-alumina: Efficient photocatalytic oxidation of benzyl alcohols

Manolis D. Tzirakis [a], Ioannis N. Lykakis [a], George D. Panagiotou [b], Kyriakos Bourikas [b], Alexis Lycourghiotis [b], Christos Kordulis [b,c,*], Michael Orfanopoulos [a,*]

[a] *Department of Chemistry, University of Crete, Iraklion, Voutes 71003, Crete, Greece*
[b] *Department of Chemistry, University of Patras, GR 26500, Patras, Greece*
[c] *Institute of Chemical Engineering and High Temperature Chemical Processes (FORTH/ICE-HT), P.O. Box 1414, GR 265 00, Patras, Greece*

Received 17 May 2007; revised 27 September 2007; accepted 29 September 2007

Abstract

Four supported catalysts with the same tungsten loading were prepared by depositing decatungstate species $W_{10}O_{32}^{4-}$, through wet impregnation, on the surface of γ-alumina and silica at different pH values. The prepared samples were characterized using BET measurements as well as XRD, UV–vis DR, and XP spectroscopies. Higher dispersion of W(VI) oxo-species was obtained in the silica-supported catalysts compared with the corresponding alumina-supported ones. Within the same support, the dispersion was higher when the impregnation pH is lower than the point of zero charge (pzc) of the support. The decatungstate anions were present mainly on the silica surface without any modification, whereas these underwent a partial depolymerization on their deposition on the γ-alumina surface. The extent of depolymerization was less in the sample prepared at pH above pzc. These findings were explained in terms of the mode of deposition of the W(VI) species from the solution onto the support surface. The photocatalytic activity of the aforementioned catalysts, concerning the photooxidation of 1-phenylethanol, depends on the fraction of the $W_{10}O_{32}^{4-}$ supported species rather than on the W(VI) dispersion. Thus, extremely high conversions have been obtained over the silica-based catalysts and also over the γ-alumina-based catalyst prepared at relatively high pH. These catalysts also are very effective in the photooxidation of a series of secondary and primary benzyl alcohols, in which benzyl ketones and benzoic acids were formed as the only or major products, respectively. The easy separation of the solid catalyst from the reaction mixture, the high activity, selectivity, and stability as well as the retained activity in subsequent catalytic cycles, make these supported catalysts suitable for a small-scale synthesis. Based on product analysis and kinetic data on the heterogeneous oxidation of benzyl alcohols, we suggest that a hydrogen abstraction transfer (HAT) mechanism predominates with respect to an electron transfer (ET) one in these reactions.

Keywords: Decatungstate; Heterogeneous photooxidation; Benzyl alcohols; Catalysis; Silica; Alumina

1. Introduction

The main shortcoming of homogeneous catalytic processes comes from the requirement of catalyst recovery or separation. In many cases, catalyst separation from the reaction mixture is technically and/or economically unfeasible. Moreover, there is a growing need for environmentally benign catalysts in the synthesis of fine chemicals and pharmaceutical intermediates. The objective is to develop industrial chemical processes environmentally acceptable. Under these circumstances, the development of heterogeneous catalytic processes is the most suitable solution.

For catalytic oxidation, an attractive approach is the use of a solid, recyclable catalyst and environmentally friendly reagent, such as molecular oxygen as the oxidant, that is, without any other additive [1–6]. Working at room temperature and atmospheric pressure is obviously desirable. Another important aim is to achieve the highest possible yield and thus minimize

* Corresponding authors.
E-mail addresses: kordulis@chemistry.upatras.gr (C. Kordulis), orfanop@chemistry.uoc.gr (M. Orfanopoulos).

0021-9517/$ – see front matter
doi:10.1016/j.jcat.2007.09.023

the additional costs of separation and waste removal that may be a critical factor in a small-scale synthesis [7–10].

In this challenging field, a number of groups are investigating polyoxometalates (POMs) as catalysts with a significant activity in the oxidation of organic compounds [11–18]. Polyoxometalates (POMs) form a class of inorganic compounds that can be envisioned as soluble molecular semiconducting oxides. Their ability to undergo photoinduced multielectron transfer without changing their structure make them very attractive catalysts in the oxidation of organic substrates in the presence of molecular oxygen. Among POMs, decatungstate $W_{10}O_{32}^{4-}$ exhibits interesting photocatalytic properties, because its absorption spectrum partially overlaps the UV solar emission spectrum, opening the potential route for environmentally benign solar-photo assisted applications. Heterogeneous catalytic oxidation of organic substrates using $W_{10}O_{32}^{4-}$ is currently an area of intense interest. Nevertheless, only a few examples have been reported to date concerning the synthesis of heterogenized decatungstate catalysts [19–24].

The oxidation of alcohols into the corresponding aldehydes, ketones, and acids is a crucial transformation in organic chemistry with both academic and industrial relevance [25–27]. Following our previous work on the homogeneous photooxidation of aryl alkanols by decatungstate [28–30], here we present a detailed study on the heterogeneous photocatalyzed oxidation of a series of secondary and primary benzyl alcohols. To this purpose, decatungstate was deposited for the first time on silica and γ-alumina surface by wet impregnation at various pH values.

More specifically, in this work we deal with (i) the deposition, through wet impregnation, of the decatungstate species on the surface of γ-alumina and silica at different pH values (two catalysts based on silica and two based on γ-alumina were prepared); (ii) the characterization of the prepared catalysts using BET measurements, X-ray powder diffraction (XRD), UV–vis diffuse reflectance (DRS), and X-ray photoelectron (XPS) spectroscopies (in this context, the state of dispersion and the structure of the active phase and its dependence on the impregnation pH were investigated); (iii) the photooxidation of the 1-phenylethanol, used as a model compound, over the above catalysts (in this framework, the relationship between the physicochemical characteristics of the solid catalysts and its photocalytic activity is investigated); (iv) the stability, the possibility for recycling, the dependence of the photocatalytic activity on the catalyst amount, and the solvent effect on the catalyst activity with respect to the most active catalysts, one supported on silica and the other one supported on γ-alumina; (v) the catalytic behavior of the aforementioned more active catalysts regarding the heterogeneous photooxidations of a series of secondary and primary benzyl alcohols (in this context, various benzyl alcohols were synthesized, whereas the interest is mainly concentrated on the selectivity of the aforementioned more active catalysts); and (vi) the mechanism of the heterogeneous catalyzed photooxidation of benzyl alcohols.

2. Experimental

2.1. Preparation of supported decatungstate catalysts

Four catalysts were prepared by supporting tetrabutylammonium decatungstate on SiO_2 (Alfa Aesar, 99.8% (metal basis), specific surface area: 225 $m^2\,g^{-1}$, particle size: ∼325 mesh) and γ-Al_2O_3 (AKZO γ-alumina extrudates, HDS-000-1.5 mm E, specific surface area: 265 $m^2\,g^{-1}$, crushed to obtain powder with particle size ∼100 mesh). The tetrabutylammonium decatungstate was synthesized and purified following standard literature procedures [31]. The tetrabutylammonium decatungstate prepared was identified by FTIR spectroscopy [21]. The wet impregnation method was followed for the deposition of the active component on the surface of the supports. Two pH values of the impregnating solutions were selected for each support, one higher and one lower than the corresponding point of zero charge (pcz) of the supports (pzc = ∼7.5 for γ-Al_2O_3 [32] and pzc = ∼3 for SiO_2 [33]).

In preparation procedure, 0.5 g of $[Bu_4N]_4W_{10}O_{32}$ was dissolved in a spherical flask of a rotary evaporator that contained 60 mL CH_3CN and 15 mL of bi-distilled water. The pH of this solution is about 3, and it was regulated at the desired pH value (1.9 and 5.3 in the case of SiO_2; 5.2 and 9.0 in the case of γ-Al_2O_3) by adding NH_4OH or HNO_3. Then 5 g of the support (SiO_2 or γ-Al_2O_3) was added, and the pH of the suspension was regulated once again at the desired value. The suspension was left under rotation for 3 h, after which the solvents were removed by evaporation within 4 h, at 30 °C and 35 mbar. The solids obtained were dried in air at 110 °C for 24 h. The prepared samples contain 5 wt% W and are symbolized by the formula WO_x/SiO_2-Y or WO_x/Al_2O_3-Y, where Y indicates the pH value of the impregnation solution.

2.2. Preparation of benzyl alcohols

The synthetic procedures of benzyl alcohols (**1**–**15**) used as substrates in the present study, as well as ^{1}H NMR, ^{13}C NMR, and MS data, are presented in the supplementary material. The spectroscopic data of the corresponding oxidation products also are presented.

2.3. Physicochemical characterization of the supported decatungstate catalysts

Specific surface area (SSA) measurements were performed in a laboratory constructed apparatus by the three-point dynamic BET method. Pure nitrogen and helium (Air Liquide) were used as adsorption and carrier gas, respectively. A thermal conductivity detector (VICI, Valco Instruments Co., Inc.) was used for the detection of the adsorbed amount of nitrogen at a given partial pressure. The water pore volumes (PVs) of the samples were determined following the incipient wetness impregnation method.

Diffuse reflectance spectra (DRS) of the samples studied were recorded in the range of 200–800 nm at room temperature

using a UV–vis spectrophotometer (Varian Cary 3) equipped with an integration sphere. The corresponding supports were used as references for the catalytic samples.

FTIR spectrum of the tetrabutylammonium decatungstate synthesized was recorded in a Perkin–Elmer 16 PC FTIR spectrophotometer using wafer of the sample in KBr. The spectrum was recorded in the range 500–4500 cm^{-1}, with a nominal resolution of 2 cm^{-1} and averaging 10 spectra.

X-ray diffraction (XRD) patterns were obtained in the range 15°–80° (scanning rate 2° min^{-1}) with a Philips PW 1480 automated diffractometer using Cu$K\alpha$ ($\lambda = 1.4518$ Å) radiation filtered through Ni. X-ray photoelectron spectra (XPS) were recorded at room temperature in an UHV chamber (base pressure 8×10^{-10} mbar) consisting of a fast specimen entry assembly, a preparation, and an analysis chamber. The residual pressure in the analysis chamber was below 10^{-8} mbar. The latter was equipped with a hemispherical electron energy analyzer (SPECS, LH 10) and a twin-anode X-ray gun for XPS. The unmonochromatized Mg$K\alpha$ line at 1253.6 eV and a constant pass energy mode for the analyzer were used in the experiments. Pass energies of 36 and 97 eV resulted in full width at half maximum (FWHM) of 0.9 and 1.6 eV, respectively, for the $Ag3d_{5/2}$ peak of a reference foil. The binding energies were calculated with respect to the C1s peak (C–C, C–H) set at 284.6 eV.

UV–vis spectra were recorded on a Hitachi U-2001 spectrophotometer with bandwidth 195–1100 nm for determining the concentration of the $W_{10}O_{32}^{4-}$ species in solution. This determination was performed after evaluating the stability of the supported catalysts (see Section 3.3).

2.4. Photocatalytic reactions

The catalytic reactions were carried out in an open cap vial equipped with a Teflon septum. The reaction mixture was irradiated under molecular oxygen bubbling. A Variac Cermax 300-W xenon lamp ($\lambda > 300$ nm) was used. Most of the experiments used HPLC-grade acetonitrile as the solvent; however, acetone, dichloromethane, diethyl ether and ethyl acetate were also used as solvents in several experiments. The reaction mixture (4 mL) contained 0.05 M of substrate and an amount of catalyst corresponding to 5.5×10^{-4} M $[Bu_4N]_4W_{10}O_{32}$. The catalytic grains were kept in suspension by vigorous magnetic stirring. The photocatalytic reactions were carried out at 5–10 °C in an ice water bath.

During irradiation, the reaction mixture was monitored by gas chromatography and ^{1}H NMR spectroscopy. ^{1}H NMR and ^{13}C NMR spectra were recorded on a Bruker AMX 500 MHz spectrometer, in $CDCl_3$. GC analysis was conducted on a Shimadzu GC-17A equipped with a 60-m HP-5 capillary column. GC-MS analysis was performed on a Shimadzu GC MS-QP5050A apparatus equipped with a 50-m HP-5 capillary column and a 5971A MS detector. Detailed data concerning the product analysis of decatungstate-catalyzed photooxidations are presented in supplementary material.

Table 1
The catalysts prepared, their specific surface areas (SSA) and pore volumes (PV), the percentage of the tungsten atoms on their surfaces determined by XPS ($W_{s.a.}$) and the W-phase surface areas per gram of catalyst (W_{SSA})

Catalyst	SSA[a] ($m^2\ g^{-1}$)	PV[b] ($cm^3\ g^{-1}$)	$W_{s.a.}$ (%)	W_{SSA} ($m^2\ g^{-1}$)
WO_x/SiO_2-1.9	157	1.39	6.5	10.2
WO_x/SiO_2-5.3	130	1.30	7.3	9.5
WO_x/Al_2O_3-5.2	180	0.52	4.9	8.8
WO_x/Al_2O_3-9.0	120	0.46	5.3	6.4

[a] SSA of $SiO_2 = 225\ m^2\ g^{-1}$, SSA of $Al_2O_3 = 265\ m^2\ g^{-1}$.
[b] PV of $SiO_2 = 1.6\ cm^3\ g^{-1}$, PV of $Al_2O_3 = 0.65\ cm^3\ g^{-1}$.

3. Results and discussion

3.1. Catalyst characterization

3.1.1. Dispersion of the active phase

The BET, XPS, and XRD results allowed investigation of the state of dispersion of the active phase. The specific surface areas (SSAs) of the samples are summarized in Table 1. This table shows that deposition of the decatungstate salt provoked a drastic diminution of the SSAs of the supports. This likely indicates that thin pores of the supports were plugged by the deposited phase, as confirmed by a corresponding decrease in the pore volumes of the samples, also summarized in Table 1. However, the decrease in SSA and PV are relatively low in the cases where the impregnation pH used is below the pzc of the corresponding support. This indicates that better dispersion of the supported phase was achieved when the support surfaces were positively charged.

The aforementioned influence of the impregnation pH on the dispersion of the supported phase is confirmed by the XPS results presented in Table 1. In fact, based on the normalized areas of the XPS peaks of the W4f, Al2p, Si2p and O1s core electrons and the corresponding atomic sensitivity factors [34] we have calculated the percentage of the tungsten atoms on the surfaces of the catalysts prepared ($W_{s.a.}$). Assuming that the W, Al, Si, and O surface atoms occupy similar areas on the surface and by multiplying the $W_{s.a.}/100$ values with the specific surface areas of the catalysts, the SSA of the active phase (W_{SSA}) was estimated for each sample (Table 1). It can be seen that this parameter is higher when the impregnation pH is lower than the pzc of the support. The influence of the impregnation pH on the dispersion of the supported phase implies that electrostatic interactions are exerted on impregnation between the positively charged surface hydroxyls of the supports and the W-oxo anions. In effect, these interactions could be responsible for the high dispersion of the W-phase [35]. We discuss this point further later in the paper.

The XRD patterns (not presented here) of the alumina-supported samples showed no peaks assigned to the decatungstate crystallites. The only peaks observed in these patterns were due to the γ-alumina used as support. On the other hand, peaks assigned to the decatungstate crystallites were hardly detected in the SiO_2-supported catalysts, whereas XRD peaks due to the support were not detected, because silica is an amorphous

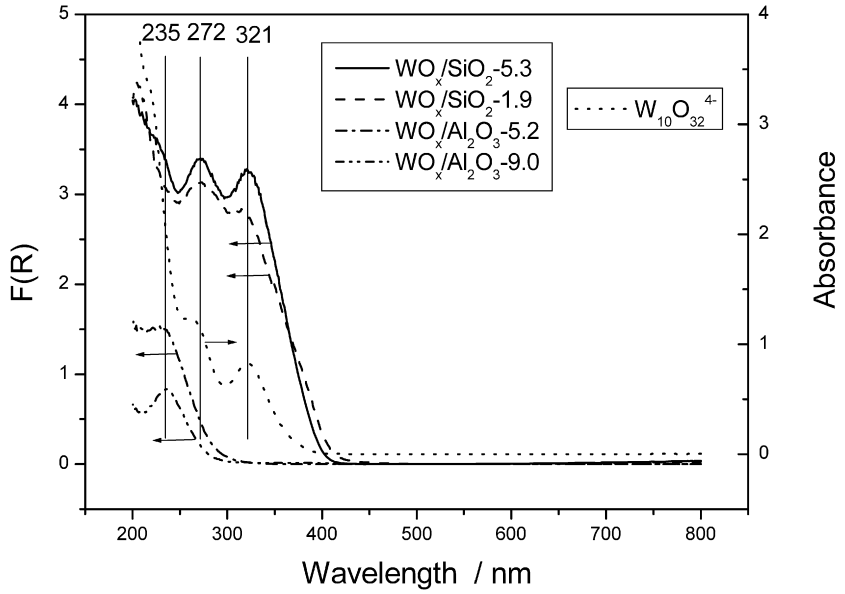

Fig. 1. The diffuse reflectance spectra of the samples prepared (WO_x/SiO_2-Y and WO_x/Al_2O_3-Y) and the absorption spectrum of $(n\mathrm{Bu_4N})_4W_{10}O_{32}$ in the impregnation solution ($W_{10}O_{32}^{4-}$).

material. The above suggest that relatively good dispersion of the supported W-phase was achieved in all cases though, as already mentioned, its magnitude depended on the impregnation pH and the support used.

3.1.2. Structure of the active phase

Fig. 1 presents the DR spectra recorded for the samples, along with the spectrum of the impregnation solution that contained dissolved tetrabutylammonium decatungstate ($W_{10}O_{32}^{4-}$). The fact that the samples did not absorb in the range 400–800 nm indicates that W-oxo species with valence <6 were not practically formed on the surface of both supports irrespective of the impregnation pH. This is in excellent agreement with our XPS results, which in all cases showed a binding energy equal to 35.0 ± 0.1 eV for the $W4f_{7/2}$ photoelectrons corresponding to W(VI) [36].

3.1.2.1. Structure of the active phase supported on γ-alumina

The absorption spectrum of impregnation solution ($W_{10}O_{32}^{4-}$) exhibited two main peaks at ∼272 and ∼321 nm. In contrast, the DR spectra of the WO_x/Al_2O_3-Y samples exhibited a single absorbance at ∼235 nm. In a previous work [37], we showed that the depolymerization of the W-oxo species is related to a blue shift of their absorbance from ∼380–400 nm observed in WO_3 with octahedral symmetry to ∼205–225 nm observed in Na_2WO_4 with tetrahedral symmetry. Thus, inspecting Fig. 1, we can conclude that the decatungstate species underwent partial depolymerization on their deposition on the alumina surface. Taking into account the impregnation method followed, a portion of the W-phase could be expected to have been deposited on the alumina surface during the 3 h equilibration of the impregnation suspension at the selected pH, whereas the remainder portion has been deposited by precipitation on the drying step due to the evaporation of the solvents.

Concerning the deposition of the W-oxo species from aqueous solutions on the γ-alumina surface during equilibration, a mechanism reported in the literature [38] proposes that at impregnation pHs > ∼4.5, the deposition occurs mainly via the monomeric WO_4^{2-} species, even though at acidic pH, the polymeric W-oxo species are predominant in the impregnation solution as it is indicated by equilibrium:

$$x\mathrm{WO_4^{2-}} + n\mathrm{H^+} \rightleftharpoons \mathrm{H}_p\mathrm{W}_x\mathrm{O}_y^{-2x+n} + [(n-p)/2]\mathrm{H_2O}. \quad (1)$$

Thus, according to the aforementioned deposition mechanism at impregnation pH near 5, the selective adsorption of the monomeric WO_4^{2-} species on the positively charged surface hydroxyls is the main deposition mode. This is illustrated by the equilibrium

$$\mathrm{AlOH_2^+} + \mathrm{WO_4^{2-}} \rightleftharpoons \mathrm{AlOH_2^+ \cdots WO_4^{2-}}. \quad (2)$$

The above adsorption shifts the equilibrium (1) to the left side promoting thus the depolymerization of decatungstate ions. At this point, it should be stressed that the surface of oxide supports are covered by hydroxyl groups when they are in contact with an electrolyte solution. These groups may be protonated or deprotonated resulting into positively and negatively charged hydroxyls, respectively. The relative concentration of the positively (negatively) charged surface hydroxyls increases (decreases) as pH decreases. Thus, at pH 5.2, which is considerably lower than the pzc = 7.5 of alumina, the positively charged hydroxyls are predominant, favoring the adsorption of the monomeric WO_4^{2-} species on the alumina surface via equilibrium (2). This in effect is in agreement with the blue shift observed in the DR spectrum of the dried WO_x/Al_2O_3-5.2 sample, as well as with the relatively high dispersion of the W-phase detected by XPS (Table 1).

On the other hand, at impregnation pH 9.0, used for the preparation of WO_x/Al_2O_3-9.0 sample, the monomeric WO_4^{2-}

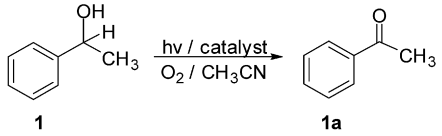

Scheme 1. Photooxidation of 1-phenylethanol (**1**) to acetophenone (**1a**).

species are predominant in the impregnation solution in accordance to the equilibrium (1), while the population of the positively charged hydroxyls on the γ-alumina surface is negligible. This is because the pzc of the γ-alumina used is ∼7.5. In view of the above the development of attractive electrostatic interactions of the monomeric WO_4^{2-} species with the support surface sites is not expectable. In fact, according to the aforementioned deposition mechanism [38] at this high pH only a small fraction of the supported W-phase could be deposited via surface reaction of the monomeric WO_4^{2-} ions with two adjacent neutral surface hydroxyls as it is illustrated by the equilibrium:

$$2\text{AlOH} + WO_4^{2-} \rightleftharpoons \text{AlO–(WO}_2\text{)–OAl} + 2OH^-. \quad (3)$$

The rest W-phase was deposited via precipitation on evaporation of the solvents. The above mechanism explains both the depolymerization of decatungstate species detected by DRS in this sample, as well as the lower W_{SSA} in comparison to that of the WO_x/Al_2O_3-5.2 sample observed by XPS (see Table 1). In fact, it is accepted that precipitation results to larger supported crystallites than adsorption [35].

3.1.2.2. Structure of the active phase supported on silica The DR spectra of the WO_x/SiO_2-Y samples are identical with the spectrum ($W_{10}O_{32}^{4-}$) of the $(n\text{Bu}_4\text{N})_4W_{10}O_{32}$ in the impregnation solution (see the absorption peaks at ∼272 and ∼321 nm; Fig. 1). This shows that the decatungstate anions are present mainly on the silica surface with no modification. However, the slightly lower intensities of the absorption peaks observed in the spectrum of WO_x/SiO_2-1.9 sample compared with those of the WO_x/SiO_2-5.3 sample probably demonstrates that a small fraction of the W-phase is deposited in the former sample via adsorption of W-oxo anions on the positively charged hydroxyls of the SiO_2 followed by depolymerization. This is in accordance with the relatively high W_{SSA} value achieved for the WO_x/SiO_2-1.9 sample (see Table 1). The above results probably show that when the deposition of $(n\text{Bu}_4\text{N})_4W_{10}O_{32}$ on the silica surface takes place by impregnation in aqueous solution at pH below pzc, a direct interaction is exerted between the W-oxo anions and the protonated surface hydroxyls of the support. However, other researchers [19,22,39] have shown that the quaternary ammonium cations of the salt interact with the support surface, and these cations may act as a bridge between the surface and the decatungstate when nonaqueous impregnation solutions are used.

3.2. Photocatalytic activity

The photocatalytic activity of the above four catalytic systems, has been assessed studying the photooxidation of 1-phenylethanol (**1**), as a model reaction. This reaction is known that, under homogeneous conditions yields acetophenone (**1a**) as the only product (Scheme 1) [28]. All of the heterogeneous catalytic reactions were carried out under the same conditions, using 0.05 M of **1** and 36.5 mg (ca. 5.5×10^{-4} M) of the supported catalyst. The kinetic curves obtained are shown in Fig. 2. In these curves, the % conversion of **1** is plotted as a function of reaction time. For comparison, the corresponding homogeneous reaction was also evaluated (dashed line in Fig. 2). When the same reaction was run in the presence of pure SiO_2 or Al_2O_3 no oxidation products were obtained. This observation indicates that the catalyst's support does not interfere to the photocatalyzed reaction. Control experiments in the absence of catalyst showed no oxidation of the substrate in the presence of molecular oxygen. In addition, no oxidation products were observed when blank experiments were run in the dark.

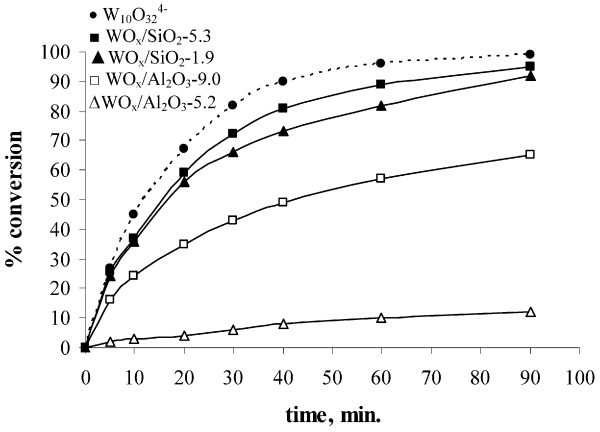

Fig. 2. Time profiles of the 1-phenylethanol photooxidation in oxygen saturated CH_3CN in the presence of $(n\text{Bu}_4\text{N})_4W_{10}O_{32}$ ($W_{10}O_{32}^{4-}$) and over the heterogeneous catalysts (WO_x/SiO_2-Y and WO_x/Al_2O_3-Y).

Table 2
Heterogeneous photooxidation of 1-phenylethanol over different supported (WO_x/SiO_2 and WO_x/Al_2O_3) decatungstate catalysts

Catalyst	Irradiation time (min)	Conversion[a] (%)	Selectivity (**1a**) (%)
$W_{10}O_{32}^{4-}$	90	99	>99
WO_x/SiO_2-1.9	90	92	>99
WO_x/SiO_2-5.3	90	95	>99
WO_x/Al_2O_3-5.2	90	12	>99
WO_x/Al_2O_3-9.0	90	65	>99

[a] Determined by ^{1}H NMR spectroscopy and gas chromatography, with error ±4% and ±1%, respectively. Naphthalene was used as internal standard.

In all cases, irradiation of **1** in acetonitrile gave the corresponding ketone **1a** as the only product. The percentage conversions for this reaction were found to be equal to 92 and 95%, respectively, over WO_x/SiO_2-1.9 and WO_x/SiO_2-5.3 samples at 90 min irradiation (Table 2). These results demonstrate that the activity of the silica-supported catalysts is surprisingly as high as that of the homogeneous precursor (Table 2). In contrast, the Al_2O_3-supported catalyst exhibited lower activity than that of the homogeneous or silica-supported catalysts. The percentage conversion over the sample WO_x/Al_2O_3-5.2 did not exceed 12%; however, a percentage conversion equal to 65% regarding

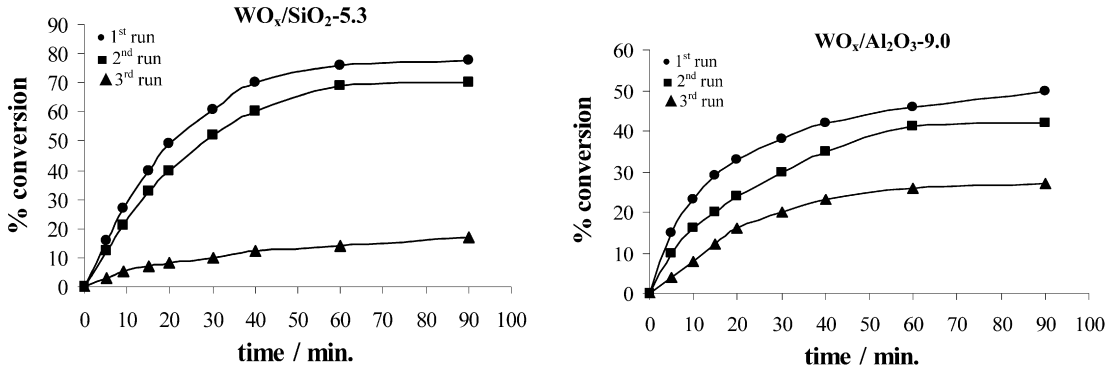

Fig. 3. Catalytic performance of recycled (a) WO_x/SiO_2-5.3 and (b) WO_x/Al_2O_3-9.0 catalysts in the heterogeneous photooxidation of **1**.

the WO_x/Al_2O_3-9.0 catalyst is quite important, demonstrating the influence of the impregnation pH (Table 2).

The activity behavior of the supported catalysts could be explained taking into account their physicochemical characteristics. More precisely, the lower activity of the WO_x/Al_2O_3-Y samples compared with the WO_x/SiO_2-Y samples could be easily attributed to the depolymerization of the decatungstate species taking place on deposition of the active phase on the alumina surface. The relatively low activity of the catalysts prepared by impregnation at pHs lower than the pzc of the corresponding supports is probably due to the stronger supported phase–support interactions developed in these cases. Such interactions stabilize the oxidation state of the supported phase. This in turn decreases the ability of the supported phase to change its oxidation state and thus to participate in the oxidation catalytic cycle needed for the heterogeneous photooxidation of 1-phenylethanol.

3.3. Stability and reusability of the catalysts

Among the various pH values and supports, the WO_x/SiO_2-5.3 and WO_x/Al_2O_3-9.0 were found to be the most efficient catalysts. Thus, we investigated the stability and reusability of these two catalysts. To test the catalysts' stability, separate solutions of WO_x/Al_2O_3-9.0 and WO_x/SiO_2-5.3 catalysts (5.5×10^{-4} M or 36.5 mg in 4 mL CH_3CN) were irradiated for 90 min under continuous oxygen bubbling at 22 ± 1 °C. Both catalysts were kept in suspension by magnetic stirring. After the irradiation experiments, the resulting solutions were centrifuged, and the UV/vis spectra of the supernatant solutions were compared with a standard solution of $(n\mathrm{Bu_4N})_4W_{10}O_{32}$ (5.5×10^{-4} M), indicating that <3% of the decatungstate had been lost from the silica or alumina.

To further confirm our results on the leaching of the catalysts, both catalysts were mixed with acetonitrile in separate solutions and stirred for 5 h at 22 ± 1 °C. Then the catalysts were filtered and removed, while 0.05 M of 1-phenylethanol was added into the filtrates. The resulting solutions were irradiated for 2 h in the presence of molecular oxygen. Only a small amount of acetophenone **1a** (4–8%) was detected by gas chromatography. The above control experiments corroborate the previous conclusion that leaching did not result in significant removal of the decatungstate catalyst from the support surface.

The above results suggest that quite strong chemical interactions occurred between supported W-oxo species and support surfaces on heating at 100 °C. Moreover, these results indicate that the contribution of the homogeneous reaction to the heterogeneously catalyzed reaction was actually negligible. Thus, we conclude that the catalytic activity of the systems studied here can be attributed almost exclusively to the heterogenized decatungstate sites.

To confirm the feasibility of catalyst recycling, **1** (0.1 M) was irradiated for 90 min in the presence of 73 mg WO_x/SiO_2-5.3 or WO_x/Al_2O_3-9.0 (11×10^{-4} M $(n\mathrm{Bu_4N})_4W_{10}O_{32}$) in oxygen-saturated CH_3CN, at 5–10 °C. The resulting solution was centrifuged, the supernatant was removed, and the solid catalyst was rinsed thoroughly 4 times with CH_3CN. The catalyst was then reused in a new catalytic cycle. The above procedure was repeated twice for each catalyst (Fig. 3).

Inspection of Fig. 3 shows that the catalysts could be reused at least twice without apparent loss of catalytic activity. The first catalytic cycle over the WO_x/SiO_2-5.3 and WO_x/Al_2O_3-9.0 samples resulted in conversion of 78 and 50%, respectively, within 90 min of irradiation. In the second cycle, the conversions were slightly decreased, to 70 and 42%, respectively. However, in the third catalytic cycle, 17 and 27% conversions were achieved within the same reaction time. Although the activity over the sample WO_x/SiO_2-5.3 was notably diminished in the third catalytic cycle, the activity over the sample WO_x/Al_2O_3-9.0 was not diminished proportionately. These results are indicative of a greater stability of the active phase when alumina was used as the catalyst support.

3.4. Effect of catalyst amount on the photocatalytic activity

To investigate the dependence of the photocatalytic activity on the amount of catalyst in the oxidation of **1,** the reaction was carried out using five different suspensions of varying catalyst concentrations. These results are illustrated in Fig. 4. Generally speaking, a higher concentration of the supported decatungstate in the reaction mixture is expected to increase the percentage conversion. As seen in Fig. 4, an increase in catalyst concentra-

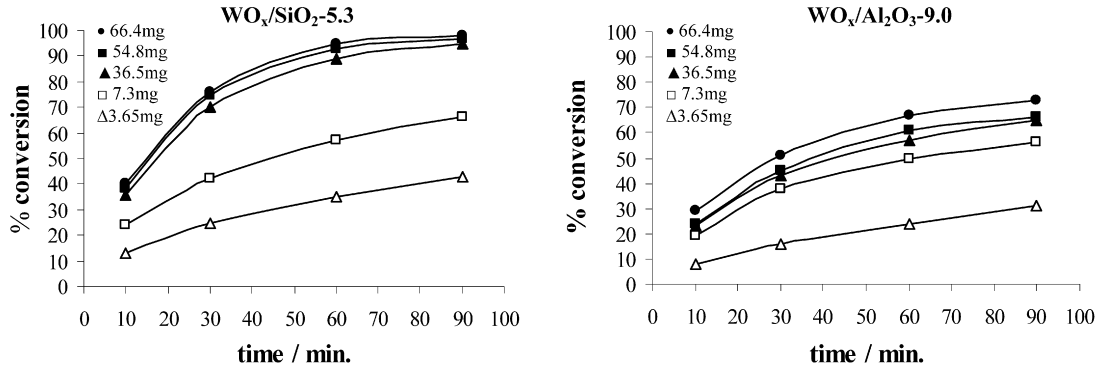

(a) (b)

Fig. 4. Time profiles of the 1-phenylethanol photooxidation catalyzed by various masses of the (a) WO_x/SiO_2-5.3 and (b) WO_x/Al_2O_3-9.0 catalysts, in oxygen saturated CH_3CN at 5–10 °C.

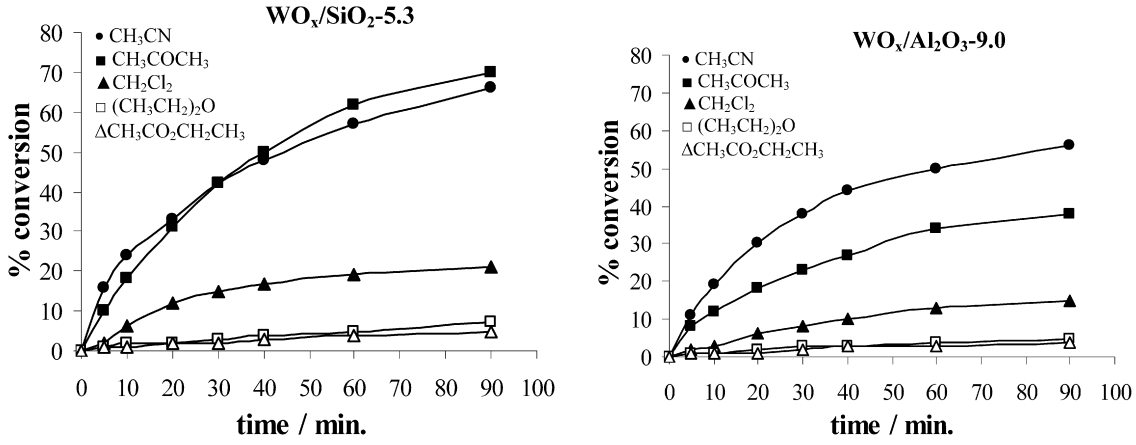

(a) (b)

Fig. 5. Time profiles of the 1-phenylethanol photooxidation over 7.3 mg of the (a) WO_x/SiO_2-5.3 and (b) WO_x/Al_2O_3-9.0 catalysts in various solvents saturated with oxygen at 5–10 °C.

tion led to higher conversions, especially in the initial stages of the reaction.

In particular, working with 3.65 mg of WO_x/SiO_2-5.3 catalyst [concentration of active phase in the reaction mixture equal to 5.5×10^{-4} M $(n\text{Bu}_4\text{N})_4\text{W}_{10}\text{O}_{32}$], almost 1 h was required for 35% completion of the reaction, compared with only 10 min when using 36.5 mg [5.5×10^{-4} M $(n\text{Bu}_4\text{N})_4\text{W}_{10}\text{O}_{32}$]. On the other hand, an additional increase in the concentration of the active phase beyond 5.5×10^{-4} M $(n\text{Bu}_4\text{N})_4\text{W}_{10}\text{O}_{32}$ did not affect the rate of the oxidation reaction to the same extent. Thus, when the concentration value of the active phase was 5.5×10^{-4} M $(n\text{Bu}_4\text{N})_4\text{W}_{10}\text{O}_{32}$, the reaction conversion reached almost maximum value (Fig. 4a). We could attribute this observation to shadow effects. In fact, as the amount of the solid catalyst increased in the reaction mixture, a continuously higher fraction of the catalyst particles could not be illuminated being in the shadow of the particles suspended in front of them. Similar and even more pronounced shadow phenomena should be operative in the case of WO_x/Al_2O_3-9.0 catalyst, as inferred by the catalytic results depicted in Fig. 4b. For example, an increase in the amount of WO_x/Al_2O_3-9.0 from 3.65 mg to 7.3 mg resulted in an increase of the final conversion from 31 to 56%, respectively. However, an even greater increase in WO_x/Al_2O_3-9.0 (from 7.3 to 36.5 mg) resulted in only a small increase in the final conversion (from 56 to 65%). Therefore, in the case of Al_2O_3-supported catalyst, the more pronounced shadow effects could be attributed to the lower transparency of the alumina compared with silica particles.

3.5. Solvent effect on the catalyst activity

Various solvents were evaluated for the catalytic photooxidation of 1-phenylethanol **1**. The kinetic results are illustrated in Fig. 5. The solvent effect on catalysts activity is actually important. Acetonitrile and acetone were found to be the most effective solvents for both catalysts (WO_x/SiO_2-5.3 and WO_x/Al_2O_3-9.0). In contrast, significantly lower conversions were achieved using dichloromethane, diethyl ether, or ethyl acetate.

3.6. Heterogeneous photooxidation of p-substituted phenyl ethanols

We extended our study of the catalytic behavior of the samples WO_x/SiO_2-5.3 and WO_x/Al_2O_3-9.0 to the *p*-substituted

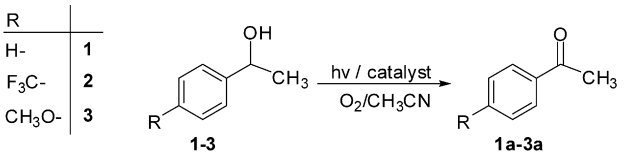

Scheme 2. Heterogeneous photooxidation of *p*-substituted phenylethanols **1**–**3**.

1-phenylethanols, 1-[4-(trifluoromethyl)phenyl]ethanol (**2**) and 1-(4-methoxyphenyl)ethanol (**3**). In this context, we studied the heterogeneous photooxidation of **2** and **3** (see Scheme 2). The synthetic procedure for these alcohols is described in supplementary materials.

All of the catalytic oxidations were carried out under the same experimental conditions, using 36.5 mg of the catalyst [concentration of the active phase 5.5×10^{-4} M $(n\mathrm{Bu_4N})_4\mathrm{W_{10}O_{32}}$] and 0.05 M of the alcohol in 4 mL CH_3CN. The activity results are compiled in Table 3, which also reports the oxidation of **1** for comparison. In all cases, the corresponding aryl ketones, **2a** and **3a**, were formed as the only products.

The kinetic results indicate that heterogenized decatungstate may be generally used for the catalytic photooxidation of benzyl alcohols. Concerning the silica-based sample, it can be seen that the effect of the *p*-substituent on the percentage conversion was rather negligible. As for the γ-alumina-based sample, as the electron-withdrawing ability of the *p*-substituent increased, the photooxidation reaction rate was accelerated. This result suggests the formation of a radical intermediate through a hydrogen atom transfer (HAT) mechanism, which is better stabilized by electron-withdrawing substituents (such as $-CF_3$).

Table 3
Results of heterogeneous photooxidation of 1-phenylethanols **1**–**3** catalyzed by WO_x/SiO_2-5.3 and WO_x/Al_2O_3-9.0 in oxygen saturated CH_3CN

Substrate	Catalyst	Irradiation time (min)	Conversion[a] (%)
1	WO_x/SiO_2-5.3	90	95
1	WO_x/Al_2O_3-9.0	90	61
2	WO_x/SiO_2-5.3	90	100
2	WO_x/Al_2O_3-9.0	90	48
2	WO_x/Al_2O_3-9.0	180	84
3	WO_x/SiO_2-5.3	90	96
3	WO_x/Al_2O_3-9.0	90	25
3	WO_x/Al_2O_3-9.0	180	39

[a] Determined by ^{1}H NMR spectroscopy and gas chromatography, with error ±4% and ±1%, respectively.

3.7. Heterogeneous photooxidation of *p*-alkyl-substituted benzyl alcohols

So far, we have reported the catalytic behavior of the WO_x/SiO_2-5.3 and WO_x/Al_2O_3-9.0 catalysts with respect to the photooxidation of *p*-substituted phenyl ethanols **1**–**3** bearing one benzylic hydrogen atom. To further probe the applicability of these heterogeneous catalytic systems in a small-scale synthesis, a series of *p*-alkyl-substituted benzyl alcohols, **4**–**10**, were oxidized under the experimental conditions described above. These substrates bear two distinguishable benzylic hydrogen atoms, one on the alcohol carbon and one on the *p*-alkyl substituent, both of which potentially can be cleaved under the photooxidation conditions. Therefore, the selectivity of the catalyst by means of preferential hydrogen abstraction can be tested. The corresponding ketone would be expected to be formed exclusively in hydrogen atom abstraction from the CH–OH carbon. On the other hand, hydrogen abstraction from the benzylic carbon of the *p*-substituent, led to the formation of dioxygenated products, as shown in Scheme 3.

Scheme 4 presents the photooxidation reactions of the *p*-alkyl-substituted benzyl alcohols. The results, summarized in Table 4, show that both catalysts tested were active in the photooxidation of benzyl alcohols **4**–**10**. Moreover, the silica-supported catalyst was more active than the alumina-supported one for all of photooxidation reactions studied.

As shown in Table 4, the photooxidation of a series of *para*-substituted benzyl alcohols **4**–**10** showed a strong preference for oxidation of the carbon that bears the hydroxy group over both WO_x/SiO_2-5.3 and WO_x/Al_2O_3-9.0 catalysts, resulting in the corresponding benzyl ketones **4a**–**10a**. 1-(4-Methylphenyl)ethanol **4** impressively illustrates this point. Similarly, alkyl-substituted phenyl ethanols **5** and **6** gave again the corresponding benzyl ketones **5a** and **6a** as the major products. However, the selectivity depends on the extent of the reaction time (results not shown). In example, for substrates **5** and **6**, at low irradiation time, high selectivities for benzyl ketones were observed (entries 3 and 5, Table 4). The same trend also was

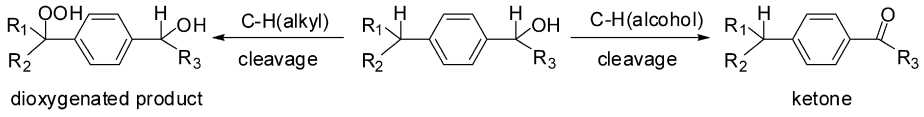

Scheme 3. Two benzylic hydrogen atoms, both potentially able to be cleaved, in the photooxidation of *p*-alkyl-substituted benzyl alcohols.

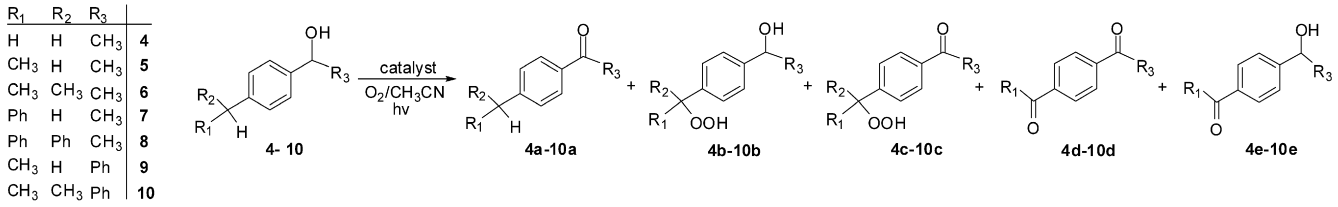

Scheme 4. Photooxidation reactions of the *p*-alkyl-substituted benzyl alcohols **4**–**10**.

Table 4
Product analysis of the heterogeneous photooxidation of aromatic alcohols **4–10** catalyzed by WO_x/SiO_2-5.3 and WO_x/Al_2O_3-9.0 in oxygen saturated CH_3CN

Entry	Substrate[a]	Catalyst	Irradiation time (min)	Conversion[b] (%)	Selectivity (%)[b,c]				
					a	**b**	**c**	**d**	**e**
1	**4**	WO_x/SiO_2-5.3	90	98	100	–	–	–	–
2	**4**	WO_x/Al_2O_3-9.0	120	97	100	–	–	–	–
3	**5**	WO_x/SiO_2-5.3	30	80	82	1	5	12	–
4	**5**	WO_x/Al_2O_3-9.0	90	70	68	12	11	9	–
5	**6**	WO_x/SiO_2-5.3	30	77	80	–	10	10	–
6	**6**	WO_x/Al_2O_3-9.0	90	41	84	11	3	2	–
7	**7**	WO_x/SiO_2-5.3	60	93	76	–	4	18	2
8	**7**	WO_x/Al_2O_3-9.0	60	73	78	–	2	14	6
9	**8**	WO_x/SiO_2-5.3	60	93	98	2	–	–	–
10	**8**	WO_x/Al_2O_3-9.0	60	44	99	1	–	–	–
11	**9**	WO_x/SiO_2-5.3	60	85	84	–	1	13	2
12	**9**	WO_x/Al_2O_3-9.0	60	63	85	–	2	9	4
13	**10**	WO_x/SiO_2-5.3	60	92	76	–	13	11	–
14	**10**	WO_x/Al_2O_3-9.0	120	88	70	–	17	13	–

[a] Arylalcohol (0.05 M) was irradiated (xenon lamp, 300 W, $\lambda > 300$ nm) in the presence of WO_x/SiO_2-5.3 and WO_x/Al_2O_3-9.0 (5.5×10^{-4} M), in 4 mL CH_3CN, at 5–10 °C.
[b] Determined by ^1H NMR spectroscopy and gas chromatography after reduction of hydroperoxides with PPh_3, with error ±4% and ±1%, respectively.
[c] See Scheme 4 for **a**, **b**, **c**, **d**, and **e**.

noted in substrates **7** and **8**, where the aforementioned selectivity, as well as the % conversion, were even higher at only 60 min of irradiation (entries 7 and 9, Table 4). In addition, the presence of a bulky phenyl group next to the benzylalcohol carbon did not change this selectivity, as demonstrated by substrates **9** and **10**. Similar selectivities also were observed in the photocatalytic oxidations of benzyl alcohols **4–10**, over WO_x/Al_2O_3-9.0. These results demonstrate a stronger and more consistent preference for hydrogen abstraction from the benzylalcohol carbon compared with the *para*-alkyl substituent of substrates **4–10**. To rationalize these results, we propose that the polar surface of the solid supports, probably favors accumulation of the polar alcohol moiety, resulting in the selective oxidation to the corresponding ketones. These results clearly demonstrate the important role of the present catalytic systems in synthetically useful oxidative transformations.

3.8. Heterogeneous photooxidation of primary benzyl alcohols

In the previous subsections, we reported on the catalytic ability of the WO_x/SiO_2-5.3 and WO_x/Al_2O_3-9.0 catalysts regarding the heterogeneous photooxidation of *secondary* benzyl alcohols. In this subsection we extend our study to the photooxidation of *primary* benzyl alcohols. This is necessary to accomplish the evaluation of these catalysts with respect to the photooxidation of benzyl alcohols. The catalytic tests were performed under the reaction conditions described previously. Benzyl alcohol **11**, 4-trifluoromethylbenzyl alcohol **12**, 4-methylbenzyl alcohol **13**, and 4-methoxybenzyl alcohol **14** (see Scheme 5) have been used as probe molecules.

Table 5 compiles the catalytic results. It may be seen that in most cases, the photooxidation of the primary benzyl alcohols **11–14** resulted in the corresponding *para*-substituted benzoic acids **11b–13b.** Only in the photooxidation of **14** with WO_x/Al_2O_3-9.0 was the corresponding aldehyde **14a** the major product. It is remarkable that in all cases, the carboxylic acid

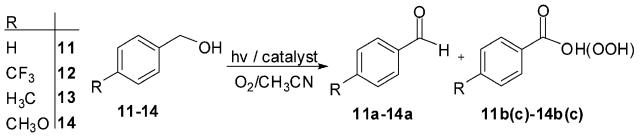

Scheme 5. Photooxidation reactions of the primary benzyl alcohols **11–14**.

Table 5
Product analysis of the heterogeneous photooxidation of benzyl alcohols **11–14** catalyzed by WO_x/SiO_2-5.3 or WO_x/Al_2O_3-9.0 in oxygen saturated CH_3CN

Substrate[a]	Catalyst	Conversion[b] (%)	Selectivity (%)[b,c]	
			a	**b, c**
11	WO_x/SiO_2-5.3	99	2	98
11	WO_x/Al_2O_3-9.0	92	3	97
12	WO_x/SiO_2-5.3	99	1	99
12	WO_x/Al_2O_3-9.0	98	2	98
13	WO_x/SiO_2-5.3	97	4	96
13	WO_x/Al_2O_3-9.0	86	5	95
14	WO_x/SiO_2-5.3	92	3	97
14	WO_x/Al_2O_3-9.0	65	56	44

[a] Benzyl alcohol (0.05 M) was irradiated (xenon lamp, 300 W, $\lambda > 300$ nm) for 90 min in the presence of WO_x/SiO_2-5.3 or WO_x/Al_2O_3-9.0 (5.5×10^{-4} M), in 4 mL CH_3CN, at 5–10 °C.
[b] Determined by ^1H NMR spectroscopy.
[c] See Scheme 5 for **a**, **b**, and **c**.

(11b–14b) versus the corresponding peroxo-compound (**11c–14c**) were formed at ratios up to 15/1. This ratio was determined by ^1H NMR spectroscopy. These results are not in agreement with recent work on the decatungstate/SiO_2-catalyzed oxidation of primary benzyl alcohols. In that study, benzyl aldehydes were reported to be the only products with no further oxidation to the carboxylic acids [40]. The observed disagreement could be related to the different method followed for catalyst preparation. In fact, the decatungstate/SiO_2 catalyst used in the latter case was prepared by entrapment of $(n\mathrm{Bu}_4\mathrm{N})_4\mathrm{W}_{10}\mathrm{O}_{32}$ into the SiO_2 matrix developed following the sol–gel procedure

involving the hydrolysis of tetraethylortho-silicate ($Si(OEt)_4$, TEOS).

3.9. Reaction mechanism

It is known that in the homogeneous decatungstate-catalyzed photooxidation, the reaction between the reactive wO intermediate with organic substrates XH may occur either by (a) hydrogen abstraction transfer (HAT) and/or (b) electron transfer (ET), according to the proposed mechanistic schemes [16,41–47] shown in Scheme 6. Both mechanisms give rise to the same 1 electron-reduced species and to the corresponding substrate-derived radical. Recent studies based on kinetic data have suggested that a HAT mechanism involves the oxidation of aryl alcohols [29,30].

To elucidate the reaction mechanism of the present heterogeneous catalysts, we performed the photooxidation reaction of **1** in the presence of 1,3,5-trimethoxybenzene (TMB), which is a well-established electron-transfer (ET) quencher. If ET occurs, TMB with $E_{1/2}$(ox) versus SCE 1.12 V [48] (oxidation potential for the 1-arylalcohols is 1.6–1.7 V, [49]) should retard the photooxidation by back-electron transfer to the **1** radical cation according to

$$\mathbf{1}^{\bullet+} + \mathrm{TMB} \rightleftharpoons \mathbf{1} + \mathrm{TMB}^{\bullet+}. \quad (4)$$

The reaction quenching plots are shown in Fig. 6. In both catalytic reactions, a significant decrease in the reaction rate can be seen, suggesting that ET likely takes part in the reaction mechanism.

To further illuminate the reaction mechanism, we investigated the WO_x/Al_2O_3-9.0 and WO_x/SiO_2-5.3 catalyzed photooxidation of 1-(4-methoxyphenyl)-2,2-dimethyl-1-propanol (**15**). This alcohol has been used as mechanistic tool for distinguishing an ET from a HAT mechanism in the side-chain oxidation of arylalkanes [49] and arylalkanols [28,49–53]. It is known that in the side-chain oxidation of aromatic alcohols, which involves an ET mechanism, a C_α–C_β bond cleavage leads to the corresponding aldehydes through a radical cation intermediate [50–53] (Scheme 7). On the other hand, a HAT mechanism leads only to the corresponding ketones [28,49].

The products likely obtained on photooxidation of **15** are presented in Scheme 8. The results obtained from these reactions are summarized in Table 6. For comparison purposes, the table also reports product analysis of the corresponding homogeneous photooxidation using $(n\mathrm{Bu_4N})_4W_{10}O_{32}$ ($W_{10}O_{32}^{4-}$) [28] and 9,10-dicyanoanthracene (DCA, a well established ET photosensitizer [48,54–58]) as catalysts. As shown in Table 6, the heterogeneous photooxidation of **15** led to the corresponding ketone **a** as the major product (80 and 82% relative yield), along with small amounts of the products **b** and **c**. This significant amount of the products **b** and **c** indicates the contribution

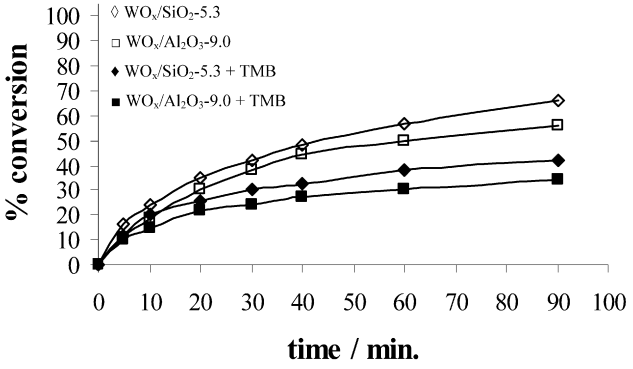

Fig. 6. Time profiles of the 1-phenylethanol photooxidation in oxygen saturated CH_3CN at 5–10 °C over 7.3 mg of the WO_x/SiO_2-5.3 and WO_x/Al_2O_3-9.0 catalysts in absence and in the presence of TMB in the reaction mixture.

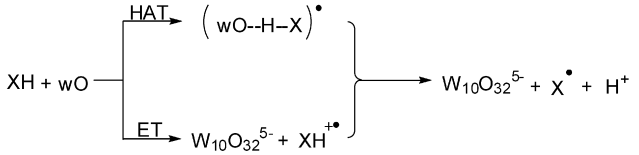

Scheme 6. Reaction of wO intermediate with organic substrates XH.

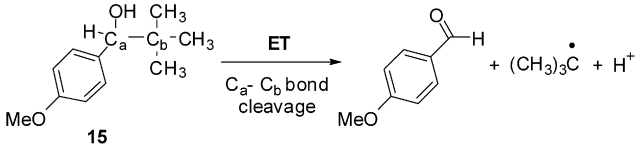

Scheme 7. Oxidation of 1-(4-methoxyphenyl)-2,2-dimethyl-1-propanol (**15**) through an electron transfer (ET) process.

Table 6
Product analysis of the 1-(4-methoxyphenyl)-2,2-dimethyl-1-propanol **15** photooxidation catalyzed by WO_x/Al_2O_3-9.0, WO_x/SiO_2-5.3, $(n\mathrm{Bu_4N})_4W_{10}O_{32}$ and DCA in oxygen saturated CH_3CN

Catalyst	Time (min)[a]	Conversion[b] (%)	Selectivity (%)[b,c]		
			a	**b**	**c**
$W_{10}O_{32}^{4-}$	20	30	97	3	–
WO_x/SiO_2-5.3	60	25	80	5	15
WO_x/Al_2O_3-9.0	60	20	82	7	11
DCA	20	30	25	65	10

[a] 1-(4-Methoxyphenyl)-2,2-dimethyl-1-propanol (0.05 M) was irradiated (xenon lamp, 300 W, $\lambda > 300$ nm) in the presence of catalyst (5.5×10^{-4} M), in 4 mL CH_3CN, at 5–10 °C.

[b] Determined by ^{1}H NMR spectroscopy with error ±1%, respectively.

[c] See Scheme 8 for **a**, **b**, and **c**.

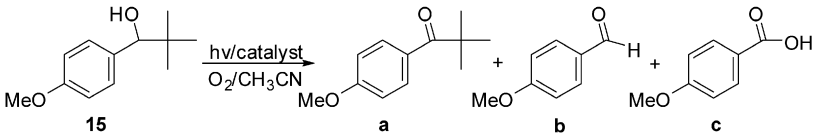

Scheme 8. Photooxidation of 1-(4-methoxyphenyl)-2,2-dimethyl-1-propanol **15** catalyzed by WA-9.0, WS-5.3, $(n\mathrm{Bu_4N})_4W_{10}O_{32}$ and DCA in oxygen saturated CH_3CN.

of an ET mechanism to the overall mechanistic pathway. In particular, in the case of an ET mechanism (DCA), products **b** and **c** would be formed as the major ones in 75% relative yield [58], whereas in the case of a HAT mechanism, product **a** would be expected to be the only one [28]. Thus, it is clear that the heterogeneous photocatalyzed oxidation of benzyl alcohols by decatungstate supported on silica and alumina proceeded via HAT and ET mechanisms, with the former as the predominant one.

4. Conclusion

Based on our findings in the present study, we can draw the following conclusions:

1. The state of dispersion of the decatungstate phase deposited on the silica and γ-alumina surface by impregnation from aqueous solutions depended on the nature of the support and also on the impregnation pH. Higher dispersion was obtained in the silica-supported catalysts compared with the corresponding alumina-supported ones. Within the same support, the dispersion was higher when the impregnation pH was lower than the pzc of the support.
2. Concerning the structure of the supported phase, we found that the decatungstate anions were present mainly on the silica surface with no modification. Only a very small fraction of the W-oxo species, deposited through electrostatic adsorption at pH below the pzc of silica, was depolymerized. In contrast, the decatungstate species underwent partial depolymerization on their deposition on the γ-alumina surface. The extent of depolymerization was smaller in the sample prepared at pH higher than pzc.
3. The differences in the state of dispersion and the structure of the deposited phase may be explained in terms of the mode of deposition of the W-oxo species from the solution onto the support surface.
4. Using 1-phenylethanol as a model compound, it was concluded that the photocatalytic activity depends on the fraction of the $W_{10}O_{32}^{4-}$-supported species rather than on the total area of the W phase. Thus, surprisingly, the activity of the silica-supported catalysts was as high as that of the homogeneous precursor, whereas the Al_2O_3-supported catalyst exhibited lower activity compared with the homogeneous or silica-supported catalysts. Moreover, within the same support, the photocatalytic activity increased with increasing impregnation pH. Extremely high conversions were obtained over the silica-based catalysts and over the γ-alumina-based catalyst prepared at relatively high pH. We further used the most active catalyst supported on silica and the most active one based on γ-alumina to investigate critical aspects of photooxidation.
5. We proved that these two supported catalysts also were very effective for the photooxidation of three series of benzyl alcohols (secondary benzyl alcohols bearing one or two distinguishable benzylic hydrogen atoms and primary benzyl alcohols). Concerning the heterogeneous photooxidation of secondary benzyl alcohols bearing two benzylic hydrogen atoms, a highly selective oxidation to the corresponding benzyl ketones was observed. Concerning the heterogeneous photooxidation of primary benzyl alcohols, we found that in most of the cases, the corresponding benzoic acids were formed selectively.
6. Based on product analysis and kinetic data, we suggest that the heterogeneous decatungstate-catalyzed oxidation of benzyl alcohols proceeded via a HAT and ET mechanism, with the former as the predominant one.
7. The easy separation from the reaction mixture, along with the high activity, selectivity, stability, and retained activity in subsequent catalytic cycles, make these supported catalysts suitable for small-scale synthesis.

Supplementary material

The online version of this article contains additional supplementary material.

Please visit DOI: 10.1016/j.jcat.2007.09.023.

References

[1] L.J. Huerta, P. Amorós, D. Beltrán-Porter, V. Cortés Corberán, Catal. Today 117 (2006) 180.
[2] C. Mateos-Pedrero, C. Cellier, P. Ruiz, Catal. Today 117 (2006) 362.
[3] C. Cellier, B. Blangy, C. Mateos-Pedrero, P. Ruiz, Catal. Today 112 (2006) 112.
[4] V. Cortés Corberán, Catal. Today 99 (2005) 33.
[5] V.P. Vislovskiy, N.T. Shamilov, A.M. Sardarly, R.M. Talyshinskii, V.Yu. Bychkov, P. Ruiz, V. Cortés Corberán, Z. Schay, Zs. Koppany, Appl. Catal. A Gen. 250 (2003) 143.
[6] L. Moens, P. Ruiz, B. Delmon, M. Devillers, Appl. Catal. A Gen. 249 (2003) 365.
[7] M. Besson, P. Gallezot, Catal. Today 57 (2000) 127.
[8] B.M. Choudary, M.L. Kantam, P.L. Santhi, Catal. Today 57 (2000) 17.
[9] B.Z. Zhan, A. Thompson, Tetrahedron 60 (2004) 2917.
[10] T. Mallat, A. Baiker, Chem. Rev. 104 (2004) 3037.
[11] C.L. Hill (Ed.), Chem. Rev. 98 (1998) 1 (a special issue of Chemical Reviews is devoted to polyoxometalates).
[12] M.T. Pope, in: Heteropoly and Isopoly Oxometallates, Springer-Verlag, Berlin, 1993.
[13] C.L. Hill, C.M. Prosser-McCartha, in: Photosensitization and Photocatalysis Using Inorganic and Organometallic Compounds, Kluwer Academic, Dordrecht, 1993.
[14] R. Neumann, M. Dahan, Nature 388 (1997) 353.
[15] C.L. Hill, C.M. Prosser-McCartha, Coord. Chem. Rev. 143 (1995) 407.
[16] C. Tanielian, Coord. Chem. Rev. 178 (1998) 1165.
[17] A. Hiskia, A. Mylonas, E. Papaconstantinou, Chem. Soc. Rev. 30 (2001) 62.
[18] C.L. Hill (Ed.), J. Mol. Catal. 262 (2007) 1 (a special issue is devoted to polyoxometalates).
[19] A. Molinari, R. Amadelli, L. Andreotti, A. Maldotti, J. Chem. Soc. Dalton Trans. (1999) 1203.
[20] A. Molinari, R. Amadelli, V. Carassiti, A. Maldotti, Eur. J. Inorg. Chem. 1 (2000) 91.
[21] A. Molinari, R. Amadelli, A. Mazzacani, G. Sartori, A. Maldotti, Langmuir 18 (2002) 5400.
[22] A. Maldotti, A. Molinari, G. Varani, M. Lenarda, L. Storaro, F. Bigi, R. Maggi, A. Mazzacani, G. Sartori, J. Catal. 209 (2002) 210.
[23] Y. Guo, C. Hu, X. Wang, Y. Wang, E. Wang, Y. Zou, H. Ding, S. Feng, Chem. Mater. 13 (2001) 4058.
[24] M. Bonchio, M. Carraro, G. Scorrano, E. Fontananova, E. Drioli, Adv. Synth. Catal. 345 (2003) 1119.

[25] M. Hudlicky, Oxidations in Organic Chemistry, Am. Chem. Soc., Washington, DC, 1990.
[26] S.V. Ley, J. Norman, W.P. Griffith, S.P. Marsden, Synthesis 7 (1994) 639.
[27] G. Tojo, M. Fernández, in: G. Tojo (Ed.), Oxidation of Alcohols to Aldehydes and Ketones: A Guide to Current Common Practice, in: Science & Business Media, Springer, 2006.
[28] I.N. Lykakis, C. Tanielian, M. Orfanopoulos, Org. Lett. 5 (2003) 2875.
[29] C. Tanielian, I.N. Lykakis, R. Seghrouchni, F. Cougnon, M. Orfanopoulos, J. Mol. Catal. 262 (2007) 170.
[30] I.N. Lykakis, C. Tanielian, R. Seghrouchni, M. Orfanopoulos, J. Mol. Catal. 262 (2007) 176.
[31] A. Chemseddine, C. Sanchez, J. Livage, J.P. Launay, M. Fournier, Inorg. Chem. 23 (1984) 2609.
[32] J. Vakros, K. Bourikas, S. Perlepes, C. Kordulis, A. Lycourghiotis, Langmuir 20 (2004) 10542.
[33] K. Bourikas, C. Kordulis, A. Lycourghiotis, Environ. Sci. Technol. 39 (2005) 4100.
[34] C.D. Wagner, L.E. Davis, M.V. Zeller, J.A. Taylor, R.H. Raymond, L.H. Gale, Surf. Interface Anal. 3 (1981) 211.
[35] K. Bourikas, C. Kordulis, A. Lycourghiotis, Catal. Rev. 48 (2006) 363.
[36] P.J.C. Chappell, M.H. Kibel, B.G. Baker, J. Catal. 110 (1998) 139.
[37] L. Karakonstantis, H. Matralis, C. Kordulis, A. Lycourghiotis, J. Catal. 162 (1996) 306.
[38] L. Karakonstantis, K. Bourikas, A. Lycourghiotis, J. Catal. 162 (1996) 295.
[39] M. Fournier, R. Thouvenot, C. Rocchiccioli-Deltcheff, J. Chem. Soc. Faraday Trans. 87 (1991) 49.
[40] S. Farhadi, M. Afshari, J. Chem. Res. S 3 (2006) 188.
[41] I. Texier, J.F. Delouis, J.A. Delaire, C. Giannotti, P. Plaza, M.M. Martin, Chem. Phys. Lett. 311 (1999) 139.
[42] I. Texier, J.A. Delaire, C. Giannotti, Phys. Chem. Chem. Phys. 2 (2000) 1205.
[43] C. Tanielian, R. Mechin, R. Seghrouchni, C. Schweitzer, Photochem. Photobiol. 71 (2000) 12.
[44] C. Tanielian, C. Schweitzer, R. Seghrouchni, M. Esch, R. Mechin, Photochem. Photobiol. Sci. 2 (2003) 297.
[45] C. Tanielian, K. Duffy, A. Jones, J. Phys. Chem. B 101 (1997) 4276.
[46] C. Tanielian, R. Seghrouchni, C. Schweitzer, Phys. Chem. A 107 (2003) 1102.
[47] D.C. Duncan, M.A. Fox, J. Phys. Chem. A 102 (1998) 102.
[48] J. Eriksen, C.S. Foote, J. Phys. Chem. 82 (1978) 2659.
[49] E. Baciocchi, M. Bietti, O. Lanzalunga, Acc. Chem. Res. 33 (2000) 243.
[50] A.L. Perrott, D.R. Arnold, Can. J. Chem. 70 (1992) 272.
[51] R. Popielarz, D.R. Arnold, J. Am. Chem. Soc. 112 (1990) 3068.
[52] E. Baciocchi, F. D'Acunzo, C. Galli, O. Lanzalunga, J. Chem. Soc. Perkin Trans. 2 (1995) 133.
[53] E. Baciocchi, M. Mattioli, R. Ruzziconi, Tetrahedron Lett. 33 (1992) 1237.
[54] C.S. Foote, Tetrahedron 41 (1985) 2221.
[55] J. Eriksen, C.S. Foote, J. Am. Chem. Soc. 102 (1980) 6083.
[56] J.W. Boyd, P.W. Schmalzl, L.L. Miller, J. Am. Chem. Soc. 102 (1980) 3856.
[57] I. Leray, M. Ayadim, C. Ottermans, H.J.L. Jiwan, J.P. Soumillion, J. Photochem. Photobiol. A 132 (2000) 43.
[58] I.N. Lykakis, S. Lestakis, M. Orfanopoulos, Tetrahedron Lett. 44 (2003) 6247.